Available online at www.sciencedirect.com

ScienceDirect

Energy Procedia 63 (2014) 532 – 541

Energy Procedia

GHGT-12

Evaluation of energetic benefit for solid-liquid phase change CO_2 absorbents

Ugochukwu Edwin Aronu*, Inna Kim, Geir Haugen

SINTEF Materials and Chemistry, P.B. 4760, N-7465 Trondheim, Norway

Abstract

A preliminary evaluation of desorption energy requirement for a precipitating system shows that precipitate formation results to a decrease in desorption energy requirement for a precipitating amino acid salt system compared to a non-precipitating one. Based on a conventional absorber-stripper configuration, only a marginal benefit may be achieved for a precipitating 5m' KSAR compared to a 30wt% MEA system. Vapour liquid solid equilibrium measurement was carried out for a newly selected precipitating system at 40 and 120 ^{o}C. This precipitating system has good absorption rate and is able to precipitate earlier in the absorption process. The measured equilibrium CO_2 partial pressure shows good temperature sensitivity and thus good potential for a significant reduction in desorption energy requirement. The cyclic capacity of this system at 10kPa CO_2 partial pressure is found to be higher than that of 30wt% MEA by 61% and by 39% for a precipitating 5m' KSAR system.

Peer-review under responsibility of the Organizing Committee of GHGT-12

Keywords: Equilibrium, precipitation, crystallization, CO_2 capture, thermodynamics, amino acid salt, MEA, absorption, desorption, phase change

1. Introduction

High regeneration energy requirement for absorbents used in CO_2 capture remains a key challenge in the capture technology process development. Precipitation is normally avoided in conventional post-combustion CO_2 absorption. Precipitation at process conditions due to solid-liquid phase change upon CO_2 absorption by some systems, however, recently has attracted attention as a possible route to energy reductions [1-4]. This is because

* Corresponding author. Tel.: +4748223272; fax: +47-73593000.
E-mail address: ugochukwu.aronu@sintef.no

Peer-review under responsibility of the Organizing Committee of GHGT-12
doi:10.1016/j.egypro.2014.11.058

precipitation of CO_2 as solid in a process will increase the CO_2 driving force into the liquid and result to increased loading capacity. Sanchez-Fernandez et al. [3] illustrated that, precipitation at process conditions can be an advantage for the amino acid salt systems through enhanced absorption and desorption. Earlier work on precipitating system was on Chilled ammonia process [5,6], but recent works on precipitating processes have been focused on precipitating carbonate and amino acid salt based systems [1,3,7]. Carbonate systems are environmentally friendly, non-volatile and stable but low CO_2 absorption rate is a key challenge. Amino acid salts on the other hand have similar performance on CO_2 reactivity and capacity to amines and some have even faster reaction rate with CO_2 [8]. They have improved environmental aspects and are salt systems thus are non-volatile. Some amino acid salts systems have however shown high desorption energy requirement when used like a conventional amine in a process [9].

Under certain process conditions amino acid salts can form solids from precipitation. This work carried out further analysis of precipitating amino acid salt studied by previous researchers ref. [1,3,4], at the defined process conditions. This paper aims to explore the benefits of process precipitation to reduce the regeneration energy requirement by finding new precipitating systems capable of early precipitation during CO_2 absorption. Previous works show 5m' KSAR as a promising amino acid salt precipitating system [3,4], but late precipitation and the consequent low reaction rate after precipitation in this system makes it less promising and necessitates further search into a more suitable precipitating system. The key activities carried out are precipitating system selection and equilibrium measurement with crystallization monitoring.

2. Materials and method

The following chemicals (CAS-nr. given in parenthesis) were used as received: ⩾ 98% pure Sarcosine (107-97-1), ⩾ 85% pure potassium hydroxide (KOH) (1310-58-3), ⩾ 99.9% pure monoethanolamine (MEA) (141-43-5). The CO_2 (purity ⩾99.99 mol %) and N_2 (purity ⩾99.999 mol %) gases were obtained from Yara Praxair. The aqueous solutions of 5m' KSAR, was prepared by adding equimolar amounts (5 mol) respectively of KOH and sarcosine to make a total aqueous solution of weight 1 kg. A new class of precipitating system; System A, B, C and D was also prepared and tested in the work. The actual solution concentrations were determined by titration.

2.1. System selection

Rapid screening experiment was used to study the precipitation behaviour and absorption rates of CO_2 into the amino acid salt solutions after a pre-selection phase. The automatic laboratory reactor Mettler Toledo LabMax® (see figure 1) presented in section 2.2 was adapted for rapid screening studies as described in ref. [1]. A 10% CO_2 CO_2-N_2 gas mixture with the flow rate of 2.5 L/min and controlled by a BRONKHORST HI-TEC N_2/CO_2 mass flow controller (model E-7100) was fed into the reactor containing a 375g absorbent solution through a stainless steel tube to avoid blockage due to precipitation while the solution is a mechanically agitated at 300 rpm. The gas bleed was condensed by cooling down to about 15 °C before entering the CO_2 analyzer. The reactor temperature was maintained at 40.0±0.1 °C through controlled cooling in the jacket. The process was terminated when the concentration of CO_2 in the outlet reached 90% of the initial CO_2 composition. FBRM and PVM probes were used to record the precipitation behavior during experiment. A liquid sample was collected and the CO_2 concentration in the liquid was measured off line by a GC Apollo 9000 Combustion TOC Analyzer and by the precipitation-titration method as described by Ma'mun et al. (2005), whereas the total alkalinity was determined by an automatic titrator Metrohm 905 Titrando. The absorption rate was calculated per kg solution as described in ref. [10]. It should be noted, that the bubble structure (relevant to the gas-liquid interfacial area) was not guaranteed to be the same in different solutions, due to variations in their interfacial tension, bubble coalescence properties and viscosity. These could affect the calculated absorption rate.

2.2. Vapour Liquid Solid Equilibrium (VLSE)

Two sets of equilibrium equipment, a LabMax® reactor and a reaction calorimeter were used to measure VLSE for the selected system. A LabMax® reactor shown in figure 1 was used to measure VLSE for the selected system C

at 40 °C. Description and operating procedure of this apparatus can be found in ref. [4]. The apparatus consists of a 1−L mechanically agitated-jacketed glass reactor equipped with temperature, pressure, pH, Particle Vision and Measurement (PVM), and Focused Beam Reflectance Measurement (FBRM) probes. This setup is also equipped with an external thermocouple, two RMS multimeters, a Bühler gas pump, an X-STREAM Enhanced XEGK - Compact Gas Analyzer, and a Bronkhorst® Hi-Tec N_2/CO_2 mass flow controller. The CO_2 concentration in the liquid phase was determined by analyzing a liquid sample taken from the reactor using a GC Apollo 9000 Combustion TOC Analyzer, while the total alkalinity concentration measurement was performed by an automatic titrator Metrohm 905 Titrando. The CO_2 partial pressure, from this setup can be calculated by use of Eq. (1).

$$p_{CO_2} = y_{CO_2}^{IR}\left[P_{tot} - \left(P_{soln}^{o} - P_{soln,IR}^{o}\right)\right] \tag{1}$$

where the $y_{CO_2}^{IR}, P_{tot}, P_{soln}^{o}$ denote CO_2 concentration in the gas phase through the IR analyser, total pressure of the system, and vapor pressure of the solution, respectively.

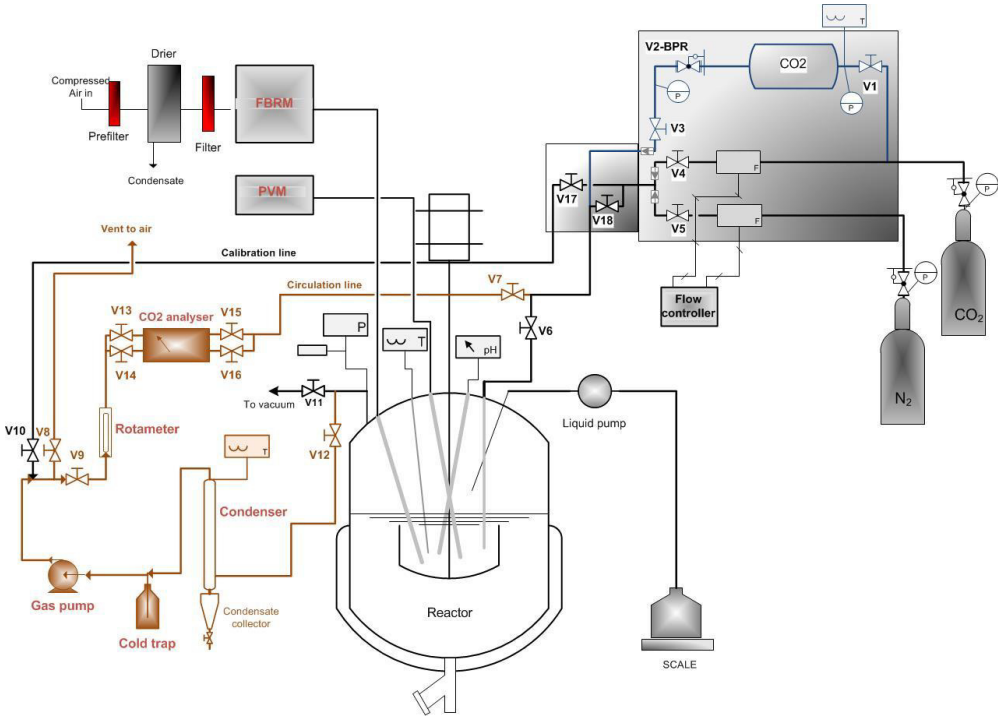

Fig. 1. Experimental setup for VLSE measurements using LabMax® reactor.

Equilibrium partial pressure of CO_2 at 120°C was calculated from the total pressure measurements in the calorimetric experiments (section 2.3) as:

$$p_{CO_2} = P_{tot} - P_{soln}^{o} \tag{2}$$

where P_{soln}^{o} is solvent pressure in the calorimeter at experimental temperature before addition of CO_2.

2.3. *Heat of CO_2 absorption*

Solvent heat of reaction with CO_2 contributes to overall desorption energy requirement. Heat of absorption of CO_2 in selected system was measured at 40 and 120 °C in a reaction calorimeter CPA-122 (Chemisens). The scheme of the experimental set-up and its operating procedure was explained in details in ref [11] and only briefly repeated

here. About 1.3 kg of the unloaded solution is charged into the 2L mechanically agitated reaction calorimeter and heated up to the desired temperatures. At equilibrium, temperature and total pressure in the calorimeter are recorded and small amount of CO_2 is added to the calorimeter through the Bronkhorst CO_2 flowmeter. The system provides a measure of the heat flow in real time. After each CO_2 loading, the system is left to reach the equilibrium before next portion of CO_2 is added, and the heat of absorption is calculated from the online heat flow and CO_2 flow data.

2.4. *Regeneration energy estimation*

Estimation of the energy demand for regeneration of the solvent is based on the work by ref [12] where they proposed two opposing limiting regimes: Heat limited regime and Stripping limited regime. Neither regime can coexist except at a specific or optimal loading where heat demand is equal between the two regimes and at a local minimum. A SINTEF in-house algorithm developed using the two regimes in a short-cut method was applied to estimate the regeneration energy requirement for both precipitating and non-precipitating systems by applying the total energy requirement as in Eq (3). It must be stressed that the short-cut method applies more adequately to a non-precipitating system since it does not take into account the heat of precipitation that is often associated with a precipitating system.

$$Q_{total} = Q_{strip} + Q_{des} + Q_{sens} \tag{3}$$

The desorption energy requirement for the precipitating amino acid salt system, 5m' KSAR, and 30wt% MEA were estimated using this short-cut method by applying the VSLE and heat of absorption data for 5m' KSAR from [4] and literature data of ref. [11] [13] for 30 wt% MEA.

3. Results and discussion

3.1. *System selection*

CO_2 absorption curves from rapid screening using the Labmax reactor for pre-selected systems are shown in figure 2 in comparison to a previously studied precipitating system, 5m' KSAR, and a conventional non-precipitating system, aqueous 30 wt% MEA.

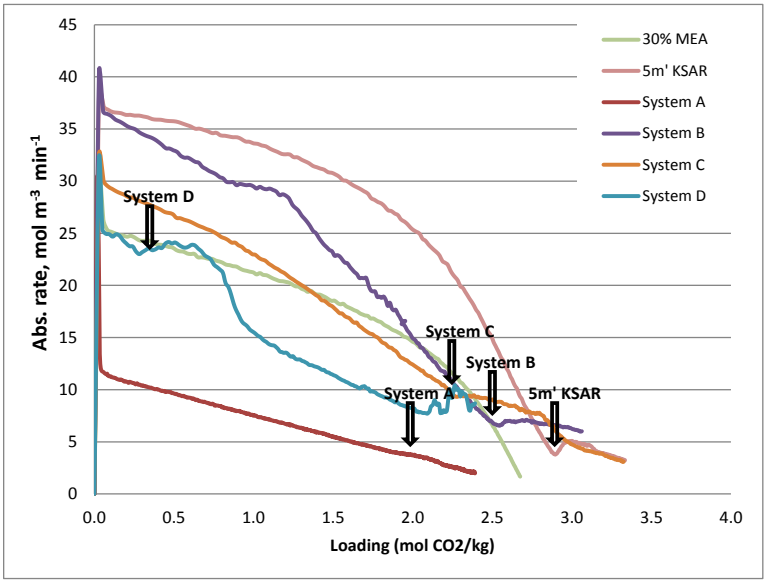

Fig. 2. CO_2 absorption curves from rapid screening using the Labmax reactor for pre-selected systems at 40 °C.

Absorption study was carried out at 40 ^{o}C. It can be observed in the figure 2, that 5m' KSAR and System A respectively have the highest and lowest absorption rates for all the systems. Black arrows show the point at which precipitation occurred in each of the systems tested. It can be observed that in all the newly tested systems except System A, precipitation occurred at higher absorption rate than 5m' KSAR this is in accordance to the objectives of this work; to develop systems that could precipitate and still maintain reasonable absorption rate. Since precipitation of CO_2 as solid in a process will increase the CO_2 driving force into the liquid and result to increased loading capacity. Among the new systems, System B and C attained high loadings with System C having the highest loading. On the other hand System B has overall higher absorption rate than System C; however, System B was found to be highly viscous. Further precipitate in System C was observed to disappear with CO_2 flashing at temperature $\leq 70^{o}$C while in System B precipitate did not dissolve completely at 80 ^{o}C. System C apparently appears to have a better overall CO_2 absorption characteristics and is therefore selected for further characterization.

3.2. *VLSE results*

VLSE equilibrium for system C was measured at 40 ^{o}C using the Labmax reactor and a reaction calorimeter. Labmax reactor was used for measurements at lower loadings at atmospheric pressure while higher loadings could have been achieved at higher pressure in the calorimeter. Equilibrium partial pressure of CO_2 at 120 ^{o}C was measured in the reaction calorimeter. Measurement at 40 ^{o}C up to loading 0.45 mol/mol was done in the Labmax reactor that has the capability for online monitoring of precipitate crystal growth and behaviour using the FBRM and PVM probes. FBRM spectra can monitor the onset of crystallization and gives information on the particle size by chord length (microns) distribution of the formed solids while PVM provides in-situ images to observe the morphology of crystals.

Figure 3 shows the results from determined VLSE for System C at 40 and 120 ^{o}C. The figure further shows the corresponding results from the FBRM counts of particles over time. The figure shows that in region A of the equilibrium curve, the particle count is $\approx$ zero indicating practically no particles in solution. Region B corresponding to loading $\approx$0.3 mol/mol show a sudden increase in particle count, fine particles, 10-50 μm for example is observed to increase to about 200; when loading is increased to 0.38 mol/mol, the particle count increases to about 800 in region C. At loading 0.45 mol/mol in region D, the particle count is seen to further rise to about 1200.

From heat of absorption measurements (see section 3.3) it is observed that heat of precipitation stopped between 0.47-0.54mol/mol. FBRM log shows that particle count increases with every loading after the first precipitation in region B; further increase in particle count is expected until the point when precipitation stops. FBRM results also show that fine particles in the range, 10-50μm are the dominant particle size in System C. It should be mentioned that determination of equilibrium point at 40^{o}C becomes more challenging and takes longer time when precipitation occurs and in particular when crystal density is high as loading increases.

PVM images in figure 4 shows that evolution of the morphology of the particles from the solution as loading increases from region A to D as shown in corresponding figure 4a to d. figure 4a shows no particle formation while figure 4b indicates the on-set of precipitation while figure 4c and d respectively shows an increasing crystal density.

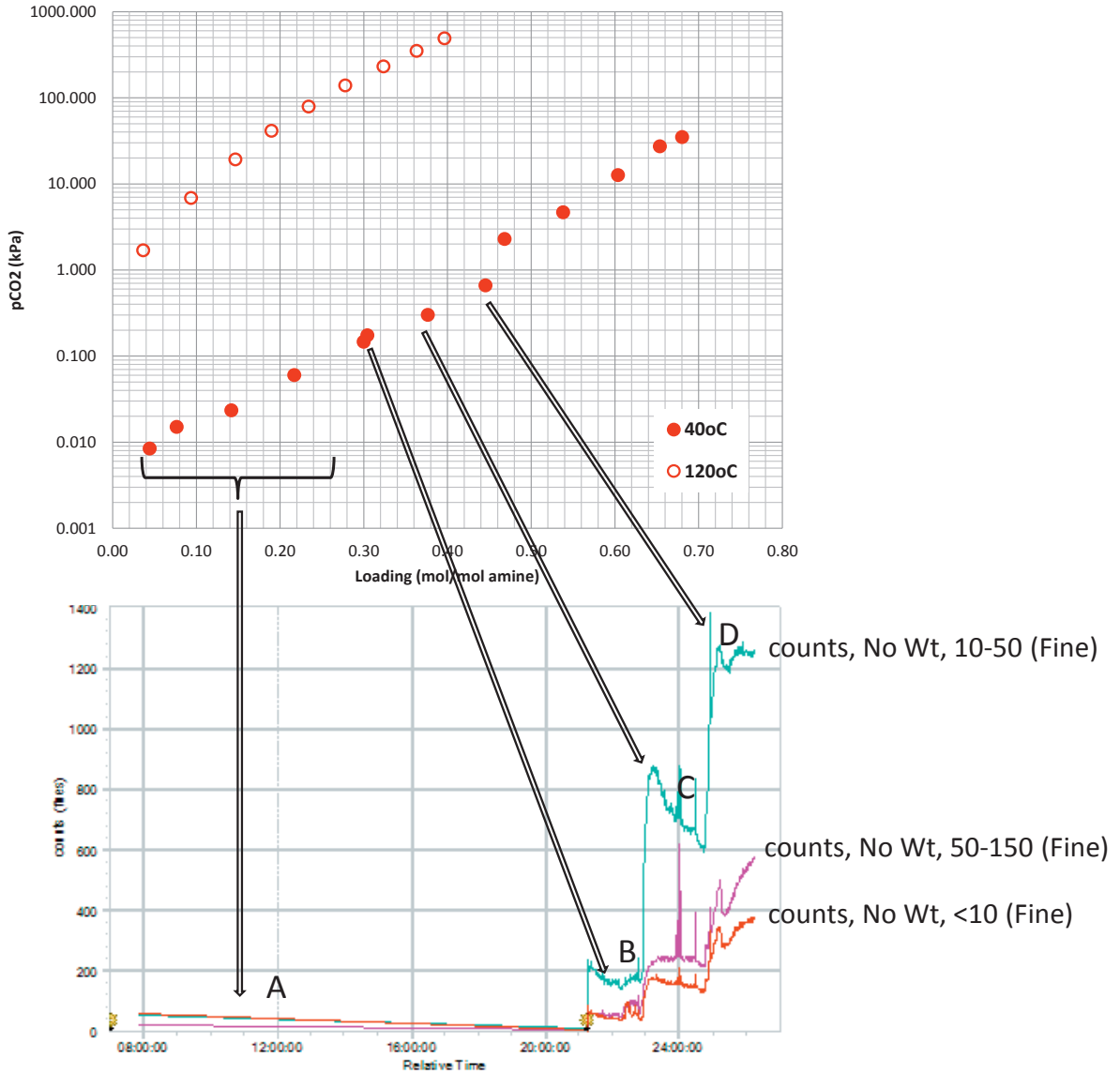

Fig. 3. Vapour liquid Solid equilibrium result for System C at 40 and 120 °C with corresponding FBRM log of particle count as loading increases at 40 °C.

2.3. Heat of absorption

Heat of absorption measured for System C at 40 and 120 °C is shown in figure 5. The figure shows the onset of precipitation (at 40 °C) by heat of precipitation resulting to increase in the heat of absorption at 40 °C after the loading point 0.29 mol/mol. VLSE measurement show that the point at which precipitation start is at loading 0.3 mol/mol (see section 3.2). Heat of absorption result shows further that the heat of absorption is temperature and loading dependent and that the value is lower at 120 °C than at 40 °C.

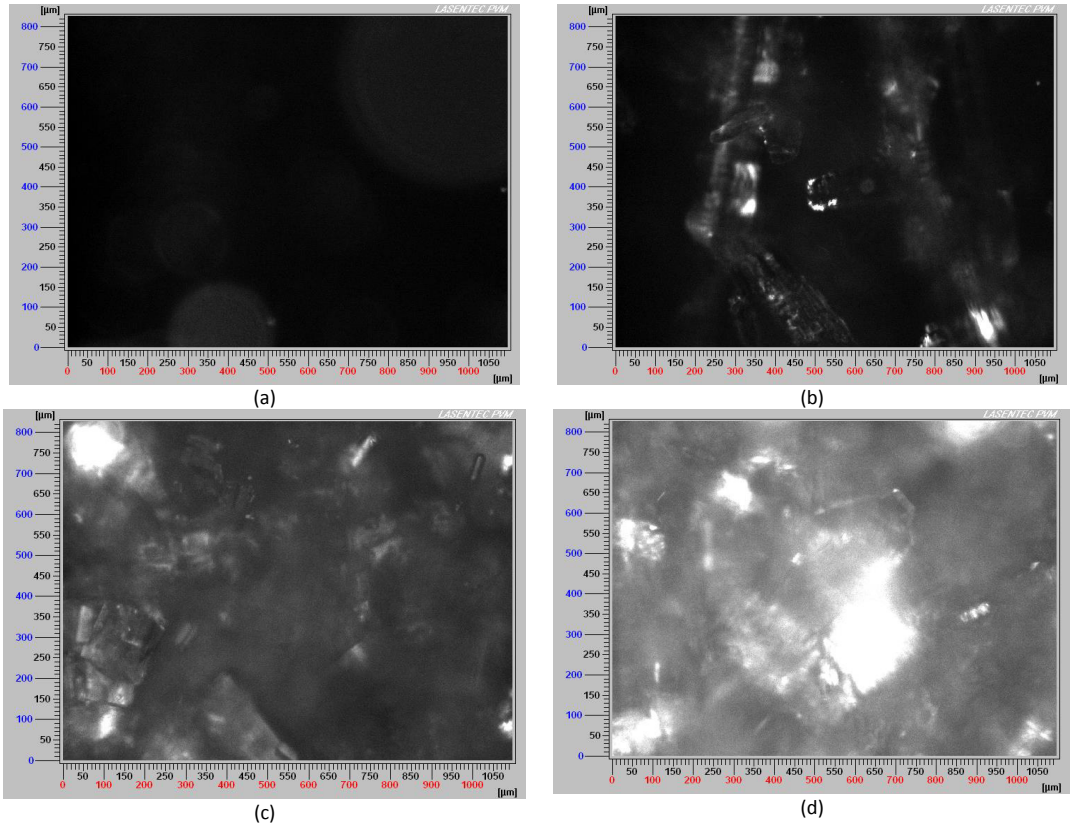

Fig. 4. Crystal morphology in System C as captured in-situ by PVM probe at 40 ºC.

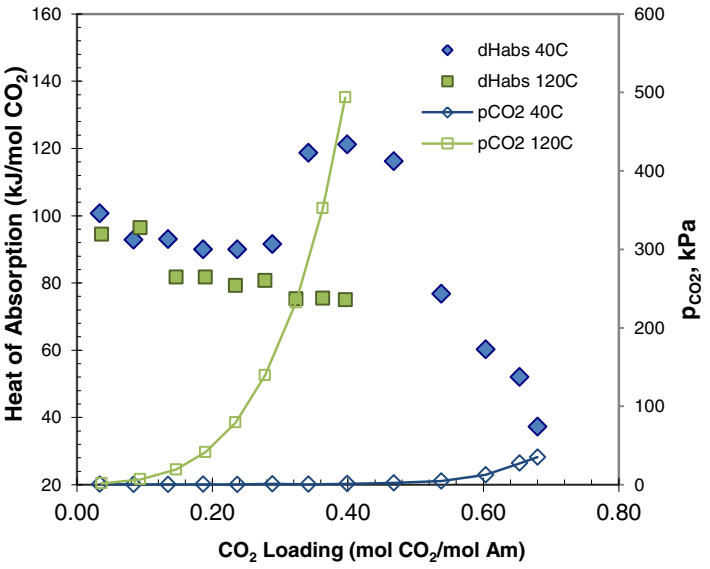

Fig. 5. Experimental heat of CO_2 absorption and pCO_2 for System C measured at 40 and 120 ºC.

2.4. Regeneration energy estimation

The shut-cut method was applied to calculate the regeneration energy requirement for 5m' KSAR and aqueous 30wt% MEA systems. This shut-cut method is mostly adapted for a non-precipitating system. It assumes a constant heat of absorption and thus does not take into account the heat of precipitation associated with a precipitating system. However, precipitating system will attain higher rich loading thus there will be compensation effect for the additional heat of precipitation but extend to which these effect will compensate each other is not known. Also the contribution of heat of precipitation to the overall regeneration energy requirement could be minimal for a precipitate that dissolves at lower temperature. At this level the shut-cut method is used as an indicator for the potential energetic benefit for all the systems using the conventional absorber-stripper configuration. Figure 6 shows a comparative result for energy numbers from a precipitating (90% equilibrium approach) and a non-precipitating (75% equilibrium approach) 5 m' KSAR system along with 30wt% MEA system at 90% equilibrium approach. At 75% equilibrium approach, 5m' KSAR will not precipitate but will have an estimated rich load of 0.52 mol/mol, [3]-[4]. The figure shows that the regeneration requirement for a 5m' KSAR is reduced significantly when precipitation is allowed to occur. The perceived drawback of the 5m' KSAR system is that precipitation occurs at high loading when the reaction rate is already very low thus full benefit of precipitation may not be easily explored. Further 5m' KSAR has very low equilibrium temperature sensitivity as can be observed in figure 6; at 120 ^{o}C and lean load of 0.25 mol/mol, pCO2 for 5m' KSAR is 2kPa while value for 30wt% MEA is 11kPa. A comparison of the precipitating 5m' KSAR with 30wt% MEA shows only a marginal reduction in energy number for a precipitating system.

The search for a new precipitating system in this work is anchored on these perceived drawbacks for the precipitating 5m' KSAR. VLSE result for the selected System C is plotted in figure 7 with 30% MEA and 5m' KSAR. Figure 2 and 3 respectively shows that precipitation was achieved at higher absorption rate and lower loading in System C than 5m' KSAR thus allowing the benefit of precipitation to be better explored. The equilibrium curves at 40 and 120oC shows that System C has the highest equilibrium temperature sensitivity, it also has better initial absorption rate that 30% MEA (see figure 2).

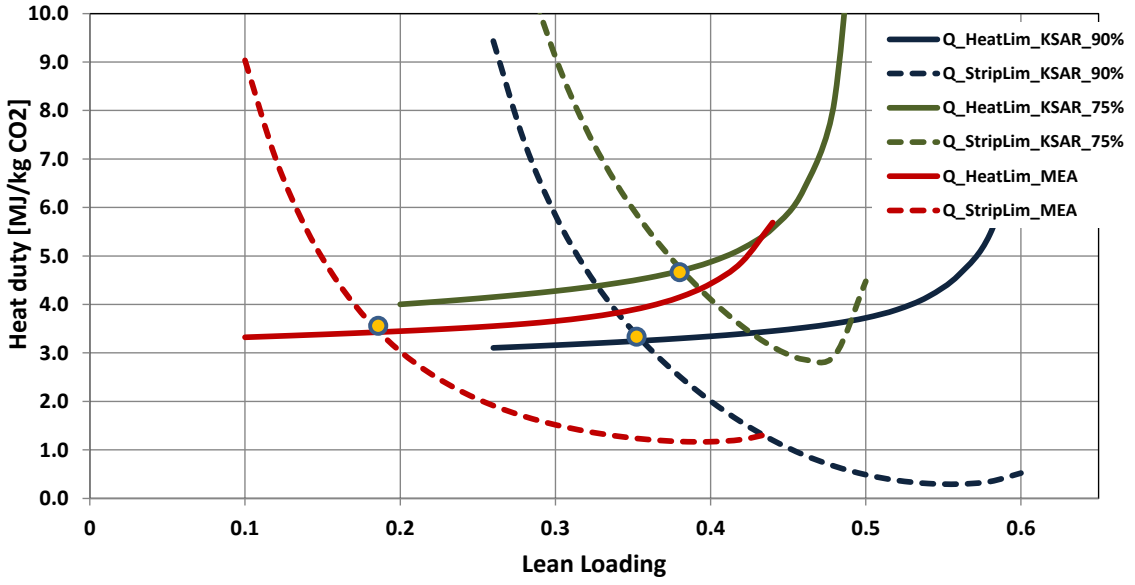

Fig. 6. Desorption energy requirement for a precipitating and non-precipitating KSAR system in comparison with 30wt% MEA estimated using a *short-cut* method.

A cyclic capacity analysis, estimated at 10kPa CO_2 partial pressure as shown in figure 7 shows that System C attains a rich and lean loading of 0.6 and 0.1 mol/mol representing a cycle capacity of 0.5 at this condition while cycle capacities for 30% MEA and 5m' KSAR a respectively 0.31 and 0.36. These represent a 61% and 39% increase in cyclic capacity compared to 30% MEA and 5m' KSAR systems respectively. System C thus shows potential for an overall improved performance for CO_2 capture process with better energy savings. The full implication of heat of precipitation for this system is unknown, however ref [7] has demonstrated that even with heat of precipitation, a precipitating system is able to attain a significantly lower regeneration energy requirement than conventional amine. Further, the precipitate in this system dissolves at temperature ≤ 70°C, thus a low grade/waste heat will be sufficient to dissolve the crystals. System C is therefore recommended for further characterization.

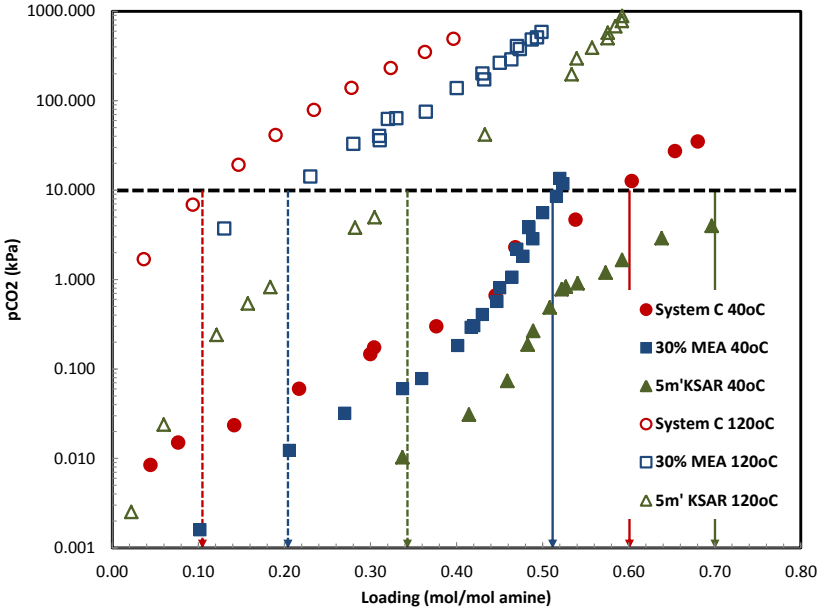

Fig. 7. Cyclic capacity estimation from equilibrium data of System C, 30wt% MEA [13] and 5m' KSAR [4] for a gas stream with 10kPa CO_2 partial pressure.

4. Conclusion

Evaluation of desorption energy requirement for a precipitating amino acid salt shows that precipitate formation results to a substantial decrease in energy number for a precipitating system compared to a non-precipitating amino acid salt system. For a precipitating amino acid salt 5m' KSAR, desorption energy requirement estimation using a shut-cut method shows that only a marginal energetic benefit may be achieved from this system compared to 30wt% MEA system under the defined processes condition with a conventional absorber-stripper configuration. A new precipitating system, System C, presented in this work has good absorption rate and is able to precipitate earlier in the absorption process. The equilibrium data shows good equilibrium temperature sensitivity and thus shows very good potential for a significant reduction in desorption energy requirement. The cyclic capacity of System C at 10kPa CO_2 partial pressure is found to be higher than that of 30wt% MEA by 61% and by 39% for a precipitating 5m' KSAR system.

Acknowledgements

This publication has been produced with support from the BIGCCS Centre, performed under the Norwegian research program Centres for Environment-friendly Energy Research (FME). The authors acknowledge the following partners for their contributions: Aker Solutions, ConocoPhilips, Det Norske Veritas AS, Gassco AS, Hydro Aluminium AS, Shell Technology AS, Statkraft Development AS, Statoil Petroleum AS, TOTAL E&P Norge AS, GDF SUEZ E&P Norge AS and the Research Council of Norway (193816/S60).

References

[1] Ma X. Precipitation in carbon dioxide capture processes. PhD Thesis, Norwegian University of Science and Technology, 2014.
[2] Sanchez-Fernandez E, Mercader F d M, Misiak K, van der Ham L, Linders M, Goetheer E. New Process Concepts for CO2 Capture based on Precipitating Amino Acids. Energy Procedia 2013, 37, 1160-1171.
[3] Aronu UE, Ciftja AF, Kim I, Hartono, A, Understanding Precipitation in Amino Acid Salt systems at Process Conditions, Energy Procedia,2013 Volume 37, 233-240.
[4] Ma'mun S, Kim I. Selection and characterization of phase-change solvent for carbon dioxide capture: precipitating system. Energy Procedia 2013, 37, 331-339.
[5] Gal E, Ultra cleaning of combustion gas including the removal of CO2. WO Patent 2006022885, 2006
[6] Darde V, Thomsen K van Well W J M, Stenby, E H. Chilled ammonia process for CO2 capture Energy Procedia, 2009, 1(1), 1035-1042.
[7]Lu Y. Bench-Scale Development of a Hot Carbonate Absorption Process with Crystallization-Enabled High Pressure Stripping for Post-Combustion CO2 Capture, Preliminary Techno-Economic Study Results and Methodology, University of Illinois, 2014
[8]Aronu UE. Amine and amino acid absorbents for CO2 capture. PhD Thesis. Norwegian University of Science and Technology. 2011.
[9]Knuutila H, Aronu UE, Kvamsdal HM, Chikukwa A. Post combustionCO2 capture with an amino acid salt. Energy Procedia, 2011, Volume 4, 1550 – 1557.
[10]Aronu U E, Hoff, K A, Svendsen, H F, CO2 capture solvent selection by combined absorption-desorption analysis. Chemical Engineering Research and Design 2011, 89(8), 1197-1203.
[11] Kim I, Svendsen HF. Heat of absorption of carbon dioxide (CO2) in monoethanolamine (MEA) and 2-(aminoethyl)ethanolamine (AEEA) solutions. Ind Eng Chem Res 2007; 46: 5803 09.
[12]Blauwhoff PMM, Kamphuis B, Van Swaaij WPM, Westerterp KR. Absorber Design in Sour Natural Gas Treatment Plants: Impact of Process Variables on Operation and Economics. Chemical Engineering and Processing: Process Intensification 1985, Volume 19, Issue 1, 1-25.
[13] Aronu UE, Gondal S, Hessen ET, Haug-Warberg T, Hartono A, Hoff KA, Svendsen HF. Solubility of CO2 in 15, 30, 45, and 60 mass% MEA from 40°C to 120°C and model representation using the extended UNIQUAC framework. Chemical Engineering Science 2011, 66(24), 6393-6406.